

## Joule Heating Effect on the Coupling of Conduction with Magnetohydrodynamic Free Convection Flow from a Vertical Flat Plate

M. A. Alim<sup>1</sup>, Md. M. Alam<sup>2</sup>, Abdullah-Al-Mamun<sup>3</sup>

<sup>1</sup>Department of Mathematics  
Bangladesh University of Engineering and Technology  
Dhaka-1000, Bangladesh  
maalim@math.buet.ac.bd

<sup>2</sup>Department of Mathematics  
Dhaka University of Engineering and Technology  
Gazipur-1700, Bangladesh

<sup>3</sup>School of Science and Engineering  
United International University  
Dhaka-1209, Bangladesh

**Received:** 19.08.2006 **Revised:** 12.05.2007 **Published online:** 31.08.2007

**Abstract.** The present work describes the effect of magnetohydrodynamic (MHD) natural convection flow along a vertical flat plate with Joule heating and heat conduction. The governing boundary layer equations are first transformed into a non-dimensional form and resulting nonlinear system of partial differential equations are then solved numerically by using the implicit finite difference method with Keller box scheme. The results of the skin friction co-efficient, the surface temperature distribution, the velocity and the temperature profiles over the whole boundary layer are shown graphically for different values of the Prandtl number  $Pr$  ( $Pr = 1.74, 1.00, 0.72, 0.50, 0.10$ ), the magnetic parameter  $M$  ( $M = 1.40, 0.90, 0.50, 0.10$ ) and the Joule heating parameter  $J$  ( $J = 0.90, 0.70, 0.40, 0.20$ ). Numerical values of the skin friction coefficients and surface temperature distributions for different values of Joule heating parameter have been presented in tabular form.

**Keywords:** free convection, conduction, Joule heating, magnetohydrodynamic.

### 1 Introduction

Free convection flow is often encountered in cooling of nuclear reactors or in the study of the structure of stars and planets. Along with the free convection flow the phenomenon of the boundary layer flow of an electrically conducting fluid up a vertical flat plate in the presence of a Joule heating term and magnetic field are also very common because of their applications in nuclear engineering in connection with the cooling of reactors. With this understanding Takhar and Soundalgekar [1] have studied the effects of viscous and

Joule heating on the problem posed by Sparrow and Cess [2], using the series expansion method of Gebhart [3]. Pozzi and Lupo [4] deal with the laminar natural convection and conduction along a flat plate. Lykoudis [5] has been investigated the behavior of the natural convection of an electrically conducting fluid in the presence of a magnetic field. Miyamoto et al. [6] studied the effect of axial heat conduction in a vertical flat plate on free convection heat transfer. The present work considers the natural convection boundary layer flow of electrically conducting fluid along a vertical flat plate of thickness  $b$  in presence of strong magnetic field and Joule heating. The transformed non-similar boundary layer equations governing the flow together with the boundary conditions based on conduction and convection were solved numerically using the implicit finite difference method together [7] with Keller box scheme [7] along with Newton's linearization approximation.

### Nomenclature

$b$	thickness of the plate	$T_b$	temperature at outer surface of the plate
$C_p$	specific heat at constant pressure	$T(x, 0)$	wall temperature of the fluid
$g$	acceleration due to gravity	$\bar{u}, \bar{v}$	dimensionless velocity components
$H_0$	applied magnetic field	$u, v$	dimensionless velocity components
$J$	Joule heating parameter	$\bar{x}, \bar{y}$	cartesian coordinates
$k_f$	thermal conductivity of the fluid	$x, y$	dimensionless cartesian coordinates
$k_s$	thermal conductivity of the solid	$\beta$	co-efficient of volume expansion
$M$	magnetic parameter	$\eta$	dimensionless similarity variable
$P$	fluid pressure	$\nu$	kinematic viscosity
$p$	coupling parameter	$\mu$	viscosity of the fluid
$Pr$	Prandtl number	$h$	dimensionless temperature
$q$	the velocity vector	$\rho$	density of the fluid
$T$	temperature of the fluid	$\sigma$	the electric conductivity

Hossain [8] studied the effect of viscous and Joule heating effects on MHD free convection flow with variable plate temperature. El-Amin [9] also analyzed the influences of both first-order and second-order resistance, due to the solid matrix of non-darcy porous medium, Joule heating and viscous dissipation on forced convection flow from a horizontal circular cylinder under the action of transverse magnetic field. To the best of our knowledge, no such study have been reported yet which deals with Joule heating effect with the coupling of conduction and MHD and the present work demonstrates the issue.

In the present investigation, Joule heating effect on the coupling of conduction with magnetohydrodynamic free convection flow from a vertical flat plate has been studied. The basic equations of motion are transformed into the local non-similarity boundary layer equations, which are solved numerically using finite difference method [7] together with the Keller box scheme [11]. The effects of the Prandtl number  $Pr$ , the magnetic parameter  $M$  and the Joule heating parameter  $J$  on the velocity and temperature fields as well as on the skin friction and surface temperature have been investigated and numerical results have been presented graphically as well as in tabular form.

## 2 Mathematical analyses

Let us consider a steady, two-dimensional laminar incompressible free convection boundary layer flow along a side of a vertical flat plate of thickness  $b$ , insulated on the edges for which pure conduction is occurred and with a temperature  $T_b$  maintained on the other side. The fluid properties are assumed to be constant in limited temperature range except for the influence of the density variations with temperature, which are considered only in body force term. The physical model and the co-ordinate system are shown in Fig. 1. The  $x$ -axis is taken along the vertical flat plate in the upward direction and the  $y$ -axis normal to the plate.

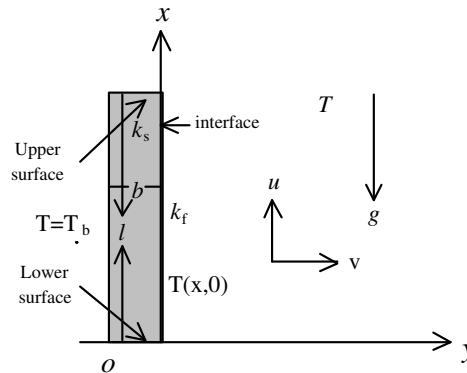


Fig. 1. Physical configuration and coordinates system.

The mathematical statement of the basic conservation laws of mass, momentum and energy for the steady viscous incompressible and electrically conducting flow has been given by Crammer and Pie [10] in vector form. Under the Boussinesq approximations the governing equations for the present problem in cartesian form can be written as

$$\frac{\partial \bar{u}}{\partial \bar{x}} + \frac{\partial \bar{v}}{\partial \bar{y}} = 0, \quad (1)$$

$$\bar{u} \frac{\partial \bar{u}}{\partial \bar{x}} + \bar{v} \frac{\partial \bar{u}}{\partial \bar{y}} = \nu \frac{\partial^2 \bar{u}}{\partial \bar{y}^2} + g\beta(T - T_\infty) - \frac{\sigma H_0^2 \bar{u}}{\rho}, \quad (2)$$

$$\bar{u} \frac{\partial T}{\partial \bar{x}} + \bar{v} \frac{\partial T}{\partial \bar{y}} = \frac{k_f}{\rho c_p} \frac{\partial^2 T}{\partial \bar{y}^2} + \frac{\sigma H_0^2}{\rho C_p} \bar{u}^2. \quad (3)$$

The appropriate boundary conditions to be satisfied by the above equations are

$$\begin{aligned} \bar{u} = 0, \quad \bar{v} = 0 \quad \text{at } \bar{y} = 0, \\ \bar{u} \rightarrow 0, \quad T \rightarrow T_\infty \quad \text{as } \bar{y} \rightarrow \infty. \end{aligned} \quad (4)$$

The coupling conditions require that the temperature and the heat flux are continuous at the solid-fluid interface and at the interface as given by Miyamoto et al. [6], we must have

$$\frac{k_s}{k_f} \frac{\partial T_{so}}{\partial \bar{y}} = \left( \frac{\partial T}{\partial \bar{y}} \right)_{\bar{y}=0}, \quad (5)$$

where  $k_s$  and  $k_f$  are the thermal conductivity of the solid and the fluid respectively. The temperature  $T_{so}$  in the solid as given by Pozzi and Lupo [4] is

$$T_{so} = T(\bar{x}, 0) - (T_b - T(\bar{x}, 0)) \frac{\bar{y}}{b}, \quad (6)$$

where  $T(\bar{x}, 0)$  is the local temperature at the solid fluid interface which is to be determined from the solutions of the equations.

We observe that the equations (1) to (3) together with the boundary conditions (4) to (5) are non-linear partial differential equations. In the following sections the solution methods of these equations are discussed details. Equations (1) to (3) may now be non-dimensionalized by using the following dimensionless dependent and independent variables:

$$\begin{aligned} x &= \frac{\bar{x}}{L}, & y &= \frac{\bar{y}}{L} d^{1/4}, & \bar{u} &= \frac{\nu}{L} d^{1/2} u, & \bar{v} &= \frac{\nu}{L} d^{1/4} v, & \frac{T - T_\infty}{T_b - T_\infty} &= \theta, \\ L &= \frac{\nu^{2/3}}{g^{1/3}}, & d &= \beta(T_b - T_\infty). \end{aligned} \quad (7)$$

Substituting expressions (7) into equations (1), (2) and (3) and in the boundary conditions (4) to (6), the following dimensionless equations are obtained.

$$\frac{\partial u}{\partial x} + \frac{\partial v}{\partial y} = 0, \quad (8)$$

$$u \frac{\partial u}{\partial x} + v \frac{\partial u}{\partial y} + Mu = \frac{\partial^2 u}{\partial y^2} + \theta, \quad (9)$$

$$u \frac{\partial \theta}{\partial x} + v \frac{\partial \theta}{\partial y} = \frac{1}{Pr} \frac{\partial^2 \theta}{\partial y^2} + Ju^2, \quad (10)$$

where  $M = \sigma H_0^2 L^2 / \mu d^{1/2}$ , the dimensionless magnetic parameter,  $Pr = \mu C_p / k_f$ , the Prandtl number,  $J = \sigma H_0^2 \nu d^{1/2} / \rho C_p (T_b - T_\infty)$ , the Joule heating parameter. The corresponding boundary conditions (4) to (6) take the following form:

$$\begin{aligned} u = v = 0, & \quad \theta - 1 = p \frac{\partial \theta}{\partial y} \quad \text{at } y = 0, \\ u \rightarrow 0, & \quad v \rightarrow 0 \quad \text{as } y \rightarrow \infty, \end{aligned} \quad (11)$$

where  $p$  is the conjugate conduction parameter given by  $p = (k_f/k_s)b/Ld^{1/4}$ . Here the coupling parameter  $p$  governs the described problem. The order of magnitude of  $p$  depends actually on  $b/L$  and  $k_f/k_s$ ,  $d^{1/4}$  being the order of unity. The term  $b/L$  attains values much greater than one because of  $L$  being small. In case of air,  $k_f/k_s$  becomes very small when the vertical plate is highly conductive i.e.  $k_s \gg 1$  and for materials,  $O(k_f/k_s) = 0.1$  such as glass. Therefore in different cases  $p$  is different but not always a small number. In the present investigation we have considered  $p = 1$  which is accepted for  $b/L$  of  $O(k_f/k_s)$ .

To solve the equations (8) to (10) subject to the boundary conditions (11), the following transformations were introduced for the flow region starting from up stream to down stream.

$$\begin{aligned}\psi &= x^{4/5}(1+x)^{-1/20}f(x,\eta), \quad \eta = yx^{-1/5}(1+x)^{-1/20}, \\ \theta &= x^{1/5}(1+x)^{-1/5}h(x,\eta).\end{aligned}\quad (12)$$

Here  $\eta$  is the dimensionless similarity variable and  $\psi$  is the stream function which satisfies the equation of continuity and  $u = \partial\psi/\partial y$ ,  $v = -\partial\psi/\partial x$  and  $h(x,\eta)$  is the dimensionless. Using the above transformation in equation (8) to (10) and simplifying, we get the following transformed non-dimensional equations.

$$\begin{aligned}f''' + \frac{16+15x}{20(1+x)}ff'' - \frac{6+5x}{10(1+x)}f'^2 - Mx^{2/5}(1+x)^{1/10}f' + h \\ = x\left(f'\frac{\partial f'}{\partial x} - f''\frac{\partial f}{\partial x}\right),\end{aligned}\quad (13)$$

$$\begin{aligned}\frac{1}{Pr}h'' + \frac{16+15x}{20(1+x)}fh' - \frac{1}{5(1+x)}f'h + Jx^{7/5}(1+x)^{-1/2}f'^2 \\ = x\left(f'\frac{\partial h}{\partial x} - h'\frac{\partial f}{\partial x}\right).\end{aligned}\quad (14)$$

In the above equations the primes denote differentiation with respect to  $\eta$ . The boundary conditions (11) then takes the following form

$$\begin{aligned}f(x,0) = f'(x,0) = 0, \quad h'(x,0) = -(1+x)^{1/4} + x^{1/5}(1+x)^{1/20}h(x,0), \\ f'(x,\infty) = 0, \quad h'(x,\infty) = 0.\end{aligned}\quad (15)$$

### 3 Method of solution

To get the solutions of the parabolic differential equations (13) and (14) along with the boundary condition (15), the implicit finite difference method [7] together with Keller-box scheme [11] has been used which is well documented by Cebeci and Bradshaw [7] and widely used by Keller and Cebeci [11] and Hossain [8].

### 4 Results and discussion

The system of non-linear ordinary differential equations (13) and (14) together with the boundary condition (15) has been solved numerically by employing implicit finite difference method together with Keller-box elimination technique. Numerical computation are carried out for Prandtl number  $Pr = 0.1, 0.5, 0.72, 1.0, 1.74$  for a wide range of the magnetic parameter  $M = 0.10, 0.50, 0.90, 1.40$  and the Joule heating parameter  $J = 0.20, 0.40, 0.70, 0.90$ .

With the above-mentioned flow parameters the results are displayed in Figs. 2 to Figs. 6 for predicting velocity profiles, temperature profiles, skin friction coefficients

and surface temperature distributions. Figs. 2(a), (b) display results for the velocity and temperature profiles, for different small values of magnetic parameter  $M$  ( $M = 0.10, 0.50, 0.90, 1.40$ ) plotted against  $\eta$  at  $Pr = 0.72$  and  $J = 0.07$ . It is seen from Fig. 2(a) that the velocity profile is influenced considerably and decreases when the value of magnetic parameter  $M$  increases. But near the surface of the plate velocity increases significantly and then decreases slowly and finally approaches to zero. The maximum values of the velocity are 0.2765, 0.3302, 0.3895 and 0.4694 for  $M = 1.40, 0.90, 0.50, 0.10$  respectively which occur at  $\eta = 1.3025$  for the first maximum value and  $\eta = 1.3693$  for others maximum values. Here we see that the velocity decreases by 41.086 % as  $M$  increases from 0.10 to 1.40. Also observed that the temperature field increases for increasing values of magnetic parameter  $M$  in Fig. 2(b). Here it is seen that the local maximum values of the temperature profiles are 0.9132, 0.8965, 0.8803, 0.8615 for  $M = 1.40, 0.90, 0.50, 0.10$  respectively and each of which occurs at the surface. Thus the temperature profiles increase by 5.67 % as  $M$  increases from 0.10 to 1.40.

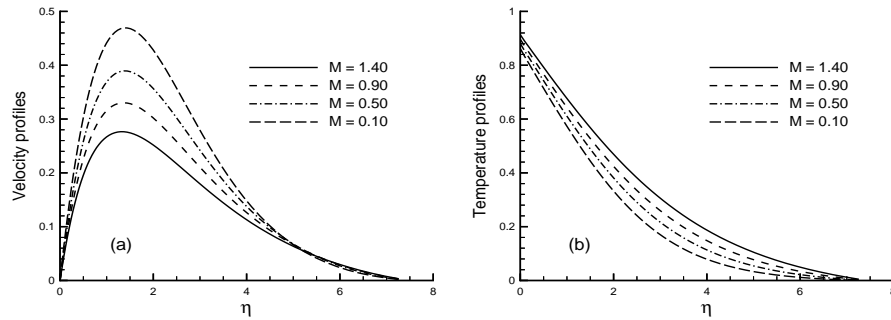


Fig. 2. (a) Velocity and (b) temperature profiles for different values of magnetic parameter  $M$  against  $\eta$  with other fixed values  $Pr = 0.72, J = 0.07$ .

Figs. 3(a) and (b) represent, respectively, the velocity and the temperature profiles for different values of the Joule heating parameter  $J$  for particular values of the Prandtl number and the magnetic parameter  $M$ . We observe from Fig. 3(a), that an increase in the Joule heating parameter  $J$ , is associated with a considerable increase in velocity profiles but near the surface of the plate the velocity increases and become maximum and then decreases and finally approaches to zero asymptotically. The maximum values of the velocity are 0.3490, 0.3412, 0.0.3299, 0.3226 for  $J = 0.90, 0.70, 0.40, 0.20$  respectively and each of which occurs at  $\eta = 1.3693$ . Here we observe that the velocity increases by 7.57 % as  $J$  increases from 0.20 to 0.90. However Fig. 3(b) shows the temperature profiles against  $\eta$  for some values of the Joule heating parameter  $J$  ( $J = 0.90, 0.70, 0.40, 0.20$ ). Clearly it is seen that the temperature distribution increases owing to increasing the values of the Joule heating parameter  $J$  and the maximum is at the adjacent of the plate wall. The local maximum values of the temperature profiles are 0.9408, 0.9302, 0.9153, 0.9059 for  $J = 0.90, 0.70, 0.40, 0.20$  respectively and each of which attains at the surface. Thus the temperature profiles increase by 3.71 % as  $J$  increases from 0.20 to 0.90.

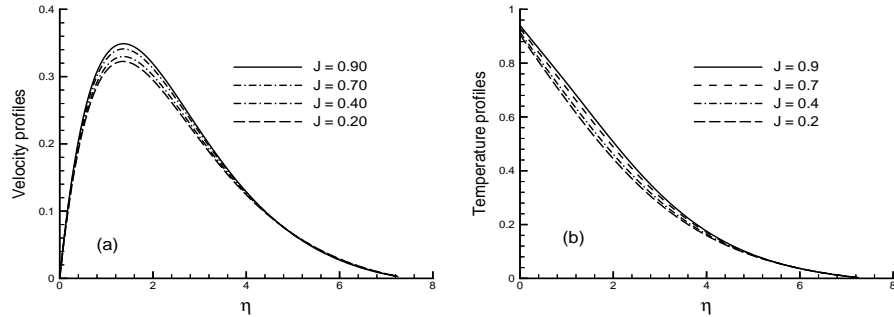


Fig. 3. (a) Velocity and (b) temperature profiles for different values of Joule heating parameter  $J$  against  $\eta$  with other fixed values  $Pr = 0.72, M = 1.0$ .

Fig. 4(a) and (b) illustrates the velocity and temperature profiles for different values of Prandtl number in presence of the magnetic parameter  $M$  and Joule heating parameter  $J$ . From Fig. 4(a), we may conclude that the velocity profile is influenced significantly and decreases when the value of the Prandtl number  $Pr$  increases. But it is seen that near the surface of the flat plate the velocity increases considerably and become maximum and then decreases slowly and finally approaches to zero. The maximum values of the velocity are 0.2373, 0.2852, 0.3156, 0.3513, 0.5169 for  $Pr = 1.74, 1.00, 0.72, 0.50, 0.10$  respectively which occur at  $\eta = 1.1752$  for the first maximum value,  $\eta = 1.3025$  for the second maximum value,  $\eta = 1.3693$  for the third maximum value,  $\eta = 1.4382$  for the fourth maximum value and at  $\eta = 1.8198$  for the last maximum value. The maximum values of the temperature are 0.8310, 0.8732, 0.8972, 0.9232, 1.0249 for  $Pr = 1.74, 1.00, 0.72, 0.50, 0.10$  respectively which occurs at the wall of the plate surface. Here it is found that the velocity and temperature profiles decrease by 54.1% and 18.92% respectively while  $Pr$  increases from 0.10 to 1.74.

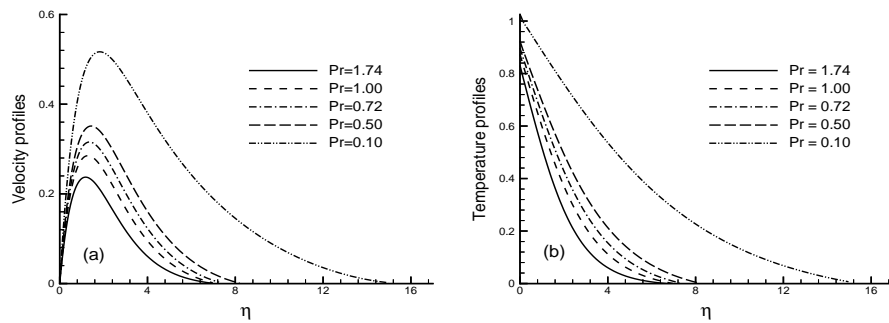


Fig. 4. (a) Velocity and (b) temperature profiles for different values of Prandtl number  $Pr$  against  $\eta$  with other fixed values  $J = 0.005, M = 1.0$ .

Figs. 5(a), (b) illustrate the variation of skin-friction  $f''(x, 0)$  and surface temperature distribution  $\theta(x, 0)$  against  $x$  for different values of magnetic parameter  $M$  ( $M = 1.40$ ,

0.90, 0.50, 0.10). It is seen from Fig. 5(a) that the skin-friction  $f''(x, 0)$  is decreases when the magnetic parameter,  $M$  increases. It is also observed in Fig. 5(b), the surface temperature  $\theta(x, 0)$  distribution increases while  $M$  increases. The value of the skin-friction  $f''(x, 0)$  decreases by 23.53 % and the surface temperature distribution  $\theta(x, 0)$  decreases by 4.33 % while the magnetic parameter  $M$  increasing from 0.10 to 1.40.

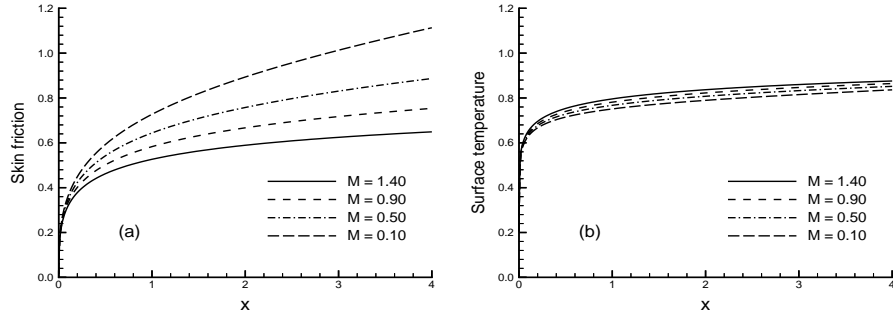


Fig. 5. (a) Skin friction and (b) surface temperature against  $x$  for different values of magnetic parameter  $M$  with fixed parameter  $Pr = 0.72, J = 0.07$ .

The effect of Prandtl number  $Pr$  ( $Pr = 1.74, 1.00, 0.72, 0.50, 0.10$ ) on the skin-friction  $f''(x, 0)$  and the surface temperature distribution  $\theta(x, 0)$  against  $x$  for the fixed parameter  $M = 1.00$  and  $J = 0.005$  is shown in Fig. 6(a), (b). It is observed that both the values of skin friction and surface temperature distribution decrease for increasing values of Prandtl number. The value of the skin-friction  $f''(x, 0)$  decreases by 13.401 % and the surface temperature distribution  $\theta(x, 0)$  decreases by 6.8 % while  $Pr$  increasing from 0.01 to 1.0.

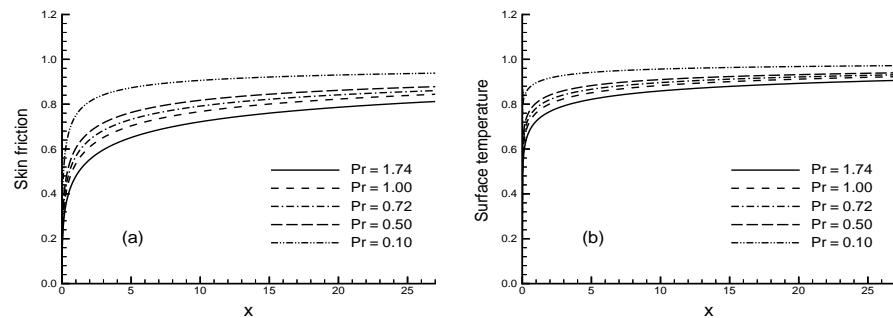


Fig. 6. (a) Skin friction and (b) surface temperature against  $x$  for different values of Prandtl number  $Pr$  with  $M = 1.0, J = 0.005$ .

In Table 1 the numerical values of the skin friction coefficient  $f''(x, 0)$  and surface temperature  $\theta(x, 0)$  against  $x$  for different for different values of Joule heating parameter  $J$  while  $M = 1.0$  and  $Pr = 0.72$ . It is observed from the table that the values of skin

friction coefficient increases rapidly at different position of  $x$  for Prandtl number  $J = 0.9, 0.7, 0.4, 0.2$ . Near the axial position  $x = 3.0$ , the rate of increase of the local shear stress coefficient is 21.67% as the Joule heating parameter  $J$  changes from 0.2 to 0.9. Furthermore, it is seen that the numerical values of the surface temperature distribution increase for increasing values of Joule heating parameter. It is also observed that the same axial position of  $x$ , the rate of increase of the surface temperature distribution is 14.23% as the Joule heating parameter  $J$  changes from 0.2 to 0.9. The rate of increase in the values of the skin-friction  $f''(x, 0)$  and the surface temperature  $\theta(x, 0)$  become much higher in the downstream than that of in the upstream values.

Table 1. Skin friction coefficient and surface temperature for different values of Joule heating parameter  $J$  against  $x$  with the fixed values of parameters  $Pr = 0.72, M = 1.0$

$x$	$J = 0.90$		$J = 0.70$		$J = 0.40$		$J = 0.20$	
	$f''(x, 0)$	$\theta(x, 0)$						
0.0000	0.0155	0.2052	0.0155	0.2052	0.0155	0.2052	0.0155	0.2052
0.3045	0.4462	0.7201	0.4446	0.7184	0.4422	0.7158	0.4406	0.7141
0.7090	0.5553	0.7851	0.5494	0.7798	0.5407	0.7721	0.5351	0.7671
1.0265	0.6146	0.8204	0.6040	0.8115	0.5889	0.7990	0.5792	0.7910
2.0369	0.7699	0.9153	0.7370	0.8901	0.6929	0.8572	0.6667	0.8381
3.0049	0.9218	1.0119	0.8541	0.9614	0.7690	0.9003	0.7221	0.8679
4.0219	1.1131	1.1384	0.9890	1.0460	0.8428	0.9428	0.7688	0.8932
5.0387	1.3568	1.3058	1.1487	1.1489	0.9175	0.9864	0.8098	0.9154
6.0502	1.6696	1.5294	1.3430	1.2779	0.9968	1.0332	0.8477	0.9361
7.1132	2.0943	1.8459	1.5967	1.4516	1.0888	1.0885	0.8862	0.9573
10.0179	3.9224	3.3321	2.6475	2.2203	1.4115	1.2880	0.9926	1.0163

## 5 Conclusions

The effects of Joule heating parameter  $J$ , magnetic parameter  $M$  and Prandtl number  $Pr$  on the natural convection flow along a vertical flat plate has been studied numerically. The transformed non-similar boundary layer equations governing the flow together with the boundary conditions based on conduction and convection were solved using the implicit finite difference method together with Keller box scheme. The coupled effect of natural convection and conduction required that the temperature and the heat flux be continuous at the interface. From the present investigation, the following conclusions may be drawn:

- The velocity distribution and the temperature distribution both are increasing for increasing value of the Joule heating parameter  $J$ .
- The velocity profile decreases and the temperature profile increases for increasing value of the magnetic parameter  $M$ .
- The skin friction and the surface temperature decrease for increasing value of the magnetic parameter  $M$ .

- The skin friction and the surface temperature decrease for increasing value of the Prandtl's number  $Pr$ .
- It has been observed that the temperature distribution over the whole boundary layer and the velocity distribution decrease with the increase of the Prandtl number  $Pr$ .

## References

1. H. S. Takhar, V. M. Soundalgekar, Dissipation effects on MHD free convection flow past a semi-infinite vertical plate, *Applied Scientific Research*, **36**(3) pp. 163–171, 1980.
2. E. M. Sparrow, R. D. Cess, The effect of magnetic field on free convection heat transfer, *Int. J. heat and Mass Transfer*, **3**(4), pp. 267–274, 1961.
3. B. Gebhart, Effects of viscous dissipation in natural convection, *J. Fluid Mech.*, **14**(2), pp. 225–232, 1962.
4. A. Pozzi, M. Lupo, The coupling of conduction with laminar natural convection along a flat plate, *Int. J. Heat Mass Transfer*, **31**(9), pp. 1807–1814, 1988.
5. P. S. Lykoudis, Natural convection of an electrically conducting fluid in the presence of a magnetic field, *Int. J. heat and Mass Transfer*, **5**(1), pp. 23–34, 1962.
6. M. Miyamoto, J. Sumikawa T. Akiyoshi, T. Nakamura, Effect of axial heat conduction in a vertical flat plate on free convection heat transfer, *Int. J. Heat Mass Transfer*, **23**(11), pp. 1545–1533, 1980.
7. T. Cebeci, P. Bradshaw, *Physical and Computational Aspects of Convective Heat Transfer*, Springer, New York, 1984.
8. M. A. Hossain, Viscous and Joule heating effects on MHD free convection flow with variable plate temperature, *Int. J. Heat and Mass Transfer*, **35**(12), pp. 3485–3487, 1992.
9. M. F. El-Amin, Combined effect of viscous dissipation and Joule heating on MHD forced convection over a non isothermal horizontal cylinder embedded in a fluid saturated porous medium, *Journal of Magnetism and Magnetic Materials*, **263**(3), pp. 337–343, 2003.
10. K. R. Cramer, S. I. Pai, *Magneto-fluid Dynamics for Engineering and Applied Physicists*, McGraw-Hill, New York, 1974.
11. H. B. Keller, T. Cebeci, Accurate numerical methods for boundary layer flows I. Two-dimensional laminar flows, in: *Proceedings of the Second Int. Conference on numerical Methods in fluid dynamics*, Springer, New York, pp. 92–100, 1971.